The Journal of Immunology

This information is current as
of September 5, 2017.

Analysis of Factor D Isoforms in Malpuech–Michels–Mingarelli–Carnevale Patients Highlights the Role of MASP-3 as a Maturase in the Alternative Pathway of Complement

Rasmus Pihl, Lisbeth Jensen, Annette G. Hansen, Ida B. Thøgersen, Stephanie Andres, Frederik Dagnæs-Hansen, Konrad Oexle, Jan J. Enghild and Steffen Thiel

---

Supplementary Material	**http://www.jimmunol.org/content/suppl/2017/08/09/jimmunol.170051 8.DCSupplemental**
Subscription	Information about subscribing to *The Journal of Immunology* is online at: http://jimmunol.org/subscription
Permissions	Submit copyright permission requests at: http://www.aai.org/About/Publications/JI/copyright.html
Email Alerts	Receive free email-alerts when new articles cite this article. Sign up at: http://jimmunol.org/alerts

Analysis of Factor D Isoforms in Malpuech–Michels–Mingarelli–Carnevale Patients Highlights the Role of MASP-3 as a Maturase in the Alternative Pathway of Complement

Rasmus Pihl,* Lisbeth Jensen,* Annette G. Hansen,* Ida B. Thøgersen,[†] Stephanie Andres,[‡] Frederik Dagnæs-Hansen,* Konrad Oexle,[§] Jan J. Enghild,[†] and Steffen Thiel*

Factor D (FD), which is also known as adipsin, is regarded as the first-acting protease of the alternative pathway (AP) of complement. It has been suggested that FD is secreted as a mature enzyme that does not require subsequent activation. This view was challenged when it was shown that mice lacking mannose-binding lectin (MBL)–associated serine protease-1 (MASP-1) and MASP-3 contain zymogenic FD (pro-FD), and it is becoming evident that MASP-3 is implicated in pro-FD maturation. However, the necessity of MASP-3 for pro-FD cleavage has been questioned, because AP activity is still observed in sera from MASP-1/3–deficient Malpuech–Michels–Mingarelli–Carnevale (3MC) patients. The identification of a novel 3MC patient carrying a previously unidentified MASP-3 G665S mutation prompted us to develop an analytical isoelectric focusing technique that resolves endogenous FD variants in complex samples. This enabled us to show that although 3MC patients predominantly contain pro-FD, they also contain detectable levels of mature FD. Moreover, using isoelectric focusing analysis, we show that both pro-FD and FD are present in the circulation of healthy donors. We characterized the naturally occurring 3MC-associated MASP-3 mutants and found that they all yielded enzymatically inactive proteins. Using MASP-3–depleted human serum, serum from 3MC patients, and *Masp1/3*$^{-/-}$ mice, we found that lack of enzymatically active MASP-3, or complete MASP-3 deficiency, compromises the conversion of pro-FD to FD. In summary, our observations emphasize that MASP-3 acts as an important maturase in the AP of complement, while also highlighting that there exists MASP-3–independent pro-FD maturation in 3MC patients. *The Journal of Immunology*, 2017, 199: 000–000.

The complement system is a key part of the innate immune system. It consists of >40 plasma proteins and surface-bound regulators that serve important roles in the defense against microbes, in cellular homeostasis, and in orchestration of the adaptive immune response (1). Complement is also involved in a number of autoimmune diseases in which the system becomes dysregulated and destructive, which has generated a growing interest for therapeutic intervention within the system (2–5). Com-

plement can be activated by three routes: the classical pathway (CP), the lectin pathway (LP), and the alternative pathway (AP). The CP and LP are mechanistically alike and rely on recognition of foreign molecular patterns by pattern recognition molecules (PRMs). In the LP, the PRMs carry serine proteases termed mannose-binding lectin (MBL)–associated serine proteases (MASPs), and these become activated from their zymogenic conformations through an intermolecular mechanism upon binding to a surface (6–8). Ultimately, this leads to cleavage of complement factors C4 and C2, thereby forming the C3 convertase C4b2a, which is shared between the LP and the CP. The subsequent cleavage of C3 exposes a thioester in the C3b fragment that covalently attaches to a nearby surface leading to opsonization.

The AP is fundamentally different from the LP and CP because it relies on the spontaneous "tick-over" of C3 to $C3(H_2O)$ by fluid-phase hydrolysis of the thioester (9). Factor B can bind $C3(H_2O)$ and form $C3(H_2O)B$ that is subsequently cleaved into the AP C3 convertase $C3(H_2O)Bb$ by factor D (FD), which has traditionally been considered the first-acting protease of the AP. Similarly, factor B also binds C3b generated by the LP or CP, and the AP therefore serves as an amplification loop that accounts for a significant proportion of the complement response regardless of the initiation route (10). FD, which is also called adipsin, is a 25-kDa protein that is predominantly synthesized in differentiated adipocytes (11–13) and is required for AP activity (14, 15). In addition, FD also serves important roles outside of complement, because it is involved in adipogenesis (16), insulin secretion (17), and obesity (13). FD is genetically encoded with a short hexameric propeptide (11), and the

*Department of Biomedicine, Aarhus University, DK-8000 Aarhus, Denmark; [†]Department of Molecular Biology and Genetics, Aarhus University, DK-8000 Aarhus, Denmark; [‡]Institute of Human Genetics, Technical University Munich, D-81675 München, Germany; and [§]Institute of Neurogenomics, Helmholtz Zentrum Munich, D-85764 Neuherberg, Germany

ORCIDs: 0000-0002-0558-0986 (S.A.); 0000-0001-7447-2252 (K.O.); 0000-0001-9292-9172 (J.J.E.).

Address correspondence and reprint requests to Rasmus Pihl, Department of Biomedicine, Aarhus University, Bartholins Allé 6, Building 1245, DK-8000 Aarhus C, Aarhus, Denmark. E-mail address: pihl@biomed.au.dk

The online version of this article contains supplemental material.

Abbreviations used in this article: AP, alternative pathway; $conv_{1/2}$, time required for converting 50% of the pro-FD substrate; CP, classical pathway; FD, factor D; IEF, isoelectric focusing; LP, lectin pathway; MAp44, MBL-associated protein 44; MASP, MBL-associated serine protease; MBL, mannose-binding lectin; 3MC, Malpuech–Michels–Mingarelli–Carnevale; NHS, normal human serum; O/N, overnight; pI, isoelectric point; PRM, pattern recognition molecule; RT, room temperature; WT, wild type.

original report of FD purification also identified a minor zymogenic FD fraction that could be activated by trypsin (18). However, subsequent studies were not able to reproduce this finding of zymogenic pro-FD, because only mature FD was purified from serum, plasma, and urine (19, 20). In addition, expression of pro-FD–encoding cDNA in CHO cells primarily yielded mature FD, whereas insect cells exclusively secrete a proenzyme that can be proteolytically activated (11, 21). These findings suggested that FD circulates without its propeptide, which might be removed intracellularly. This hypothesis was strengthened by the fact that FD exists in a self-inhibited state in the absence of its substrate, thus circumventing the need for a proenzymatic conformation, because its activity is regulated by a structural rearrangement that is induced by binding to the C3bB complex (22–24).

MASP-3 is a splice variant encoded by the *MASP1* gene together with MASP-1 and MBL-associated protein 44 (MAp44). MASP-1 and MASP-3 share their five N-terminal domains but differ by having distinct serine protease domains (25). The function of MASP-3 has long remained elusive, because it displays low catalytic activity toward a number of substrates (26, 27). Despite this, the enzyme seems to play an important role during development, as mutations clustering in exon 12 that encodes the serine protease domain of MASP-3 give rise to the oculopalatoskeletal syndrome Malpuech–Michels–Mingarelli–Carnevale (3MC), which is also called 3MC syndrome type 1 (MIM 257920) (28, 29). 3MC is an autosomal recessive syndrome that encompasses a wide range of clinical features such as dysmorphic facial features, postnatal growth retardation, and hearing loss (30). Moreover, 3MC syndrome type 2 (MIM 265050) is caused by mutations in *COLLEC11*, which encodes collectin kidney 1 (29), whereas 3MC syndrome type 3 (MIM 248340) is caused by mutations in the collectin liver 1–encoding *COLLEC10* gene (31). In this study, the term 3MC will refer to the *MASP1*-associated type 1 syndrome.

Surprisingly, it was reported that $Masp1/3^{-/-}$ mice, which are deficient in all *Masp1* splice variants, lack AP activity because of the fact that FD circulates as pro-FD, indicating that MASP-1, MASP-3, and/or MAp44 are implicated in the conversion of pro-FD into FD (32). Subsequently, it was shown that murine MASP-3 could rescue AP activity in vitro in $Masp1/3^{-/-}$ serum by mediating direct cleavage of both pro-FD and factor B (33). It was also suggested that MASP-3 was capable of performing pro-FD cleavage as a zymogen (33). Conversely, it has been shown that a zymogenic fragment of human MASP-3 was not able to cleave pro-FD, highlighting that it is currently not clear whether MASP-3 possesses zymogenicity (34). The link between MASP-3 and the AP was further supported by studies showing that neither inhibition of endogenous MASP-1 nor MASP-2 affects the cleavage of recombinant pro-FD in serum and plasma (34), whereas MASP-3 inhibition blocks pro-FD maturation (35). In contrast, it was reported that serum from MASP-1/3–deficient 3MC patients still possessed AP activity, albeit at a lower level than normal human serum (NHS) (36, 37). Furthermore, a study showed that factor H–deficient mice $(Cfh^{-/-})$ and $Cfh^{-/-}.Masp1/3^{-/-}$ mice were equally susceptible to developing AP-driven C3 glomerulopathy (38). These opposing observations led to a dispute in the field by questioning the necessity of MASP-3 for the AP. The complex nature of this issue became even more pronounced when Western blotting showed that only pro-FD was detectable in the sera from the 3MC patients that still contained AP activity (39).

The identification of a novel 3MC-causing MASP-3 mutation, described in this study, prompted us to examine the link between MASP-3 and pro-FD maturation with the aim of resolving the above-mentioned controversy. Because there are no analytical techniques that allow clear and easily reproducible separation of

endogenous FD variants, we developed a method that relies on isoelectric focusing (IEF) followed by blotting. Using this technique, we show that sera from 3MC patients predominantly contain pro-FD, but also a small proportion of mature FD. Unexpectedly, we also find that varying amounts of pro-FD are present in serum from healthy donors. To our knowledge, we further provide the first in vivo evidence of an MASP-3–specific effect on pro-FD conversion by rescuing AP activity in $Masp1/3^{-/-}$ mice by injection of MASP-3. Lastly, we combine the techniques developed throughout this study to show that the known 3MC-causing MASP-3 mutations are deleterious, because they either abolish functional expression or lead to loss of enzymatic activity.

Materials and Methods
Description of 3MC patients

The novel 3MC patient is the first child of nonconsanguineous German parents and is referred to as patient 3MC #1. At birth, the patient had subnormal weight ($z = -1.9$) and length ($z = -2.2$), which developed into postnatal growth retardation. At the age of 2 y, body length ($z = -2.4$), weight ($z = -1.9$), height ($z = -2.5$), and head circumference ($z = -2.1$) were all at the lower border of the normal range (40). Other developmental symptoms included combined cleft lip and cleft palate, which were surgically closed, a wide intercanthal distance, a short midface, and a skin elevation of 1 cm in diameter above the sacral bone. Echocardiography revealed mild (I^0) mitral valve insufficiency and patent ductus arteriosus that was surgically closed at the age of 6 mo. Ophthalmological examination indicated bilateral blepharophimosis, vascularization of the lenses, polar cataracts, retinal hyperpigmentation, as well as corneal clouding on the left eye. Neurosensory hearing deficiency was diagnosed and necessitated hearing aids. Milestones of cognitive and motor development were slightly delayed (no unaided walking before the age of 21 mo and only a few single words at the age of 26 mo). At the age of 11 wk, the patient developed pneumococcal meningitis in combination with bronchopneumonia. Five days of cefotaxime treatment led to recovery.

The present study also includes blood samples from patients 3MC #2 and #3, which are described in detail in previous publications. In short, patient 3MC #2 contains the mutation c.891 + 1G>T in intron 6 that prevents correct splicing and is described as patient 3 by Atik et al. (37). Proband 3MC #3 harbors the nonsense mutation c.870G>A (p.W290*) and is described as patient 101 in family 2 by Sirmaci et al. (28).

Preparation of recombinant proteins

Recombinant proteins were produced in FreeStyle 293-F cells cultured according to the supplier's instructions (Thermo Fisher Scientific). Transfection was conducted by adding polyethylenimine–DNA complexes to the cells, as previously described (41). Culture supernatants were harvested by centrifugation on day 4 after transfection.

To produce recombinant pro-FD, we inserted the pro-FD sequence into a pcMV6-XL4 vector. Purification of pro-FD was conducted by loading the culture supernatant on a Resource S cation exchange column (GE Healthcare) using 20 mM MES, 50 mM NaCl (pH 6) as starting buffer. Pro-FD eluted at ~275 mM NaCl when using a linear gradient over 30 column volumes, ultimately reaching 20 mM MES, 0.5 M NaCl (pH 6). The resulting pro-FD was further purified by size-exclusion chromatography using a Superdex 75 10/300 GL column (GE Healthcare) that was pre-equilibrated in TBS (10 mM Tris, 145 mM NaCl [pH 7.4]).

MASP-3 constructs were prepared according to the human sequence P48740-2 or the murine sequence P98064-2 (http://uniprot.org) and codon optimized for expression in human cells. The sequences were cloned into a pcDNA3.1/Zeo (+) vector using EcoRI and XbaI, and mutations were introduced into this wild type (WT) background (GenScript). The following human mutants were produced: W290*, R449Q, G484E, H497Y, D553N, C630R, D663Y, S664A, G665S, and G687R. Constructs encoding murine MASP-3 were generated as WT and the S669A mutant. Note that all numbering in this study includes the signal peptides. Human and murine recombinant MASP-3 were purified by loading culture supernatant containing 10 mM CaCl$_2$ on a recombinant MBL-Sepharose CL-4B column. The immobilized recombinant MBL on the column was expressed and purified, as previously reported (42). Subsequently, the column was washed with TBS, 10 mM CaCl$_2$ until a stable baseline was established. MASP-3 was eluted in 10 mM Tris, 1 M NaCl, 10 mM EDTA (pH 7.4) and dialyzed into TBS.

Generation of polyclonal anti–pro-FD and anti–MASP-3 Abs

The following processes were designed with and conducted by GenScript. Five micrograms of the peptide CPPRGRILGGREAEAH, which includes the FD propeptide, was coupled to the carrier protein keyhole limpet hemocyanin, emulsified in Freund's adjuvant, and used for immunization of a rabbit. The rabbit received a boost of the conjugate on days 14, 35, and 56 after the primary injection. IgG was purified from serum obtained after the last immunization by affinity chromatography using protein G beads. Subsequently, the IgG was passed over a column containing the immobilized peptide ILGGREAEAHARPYM that binds Abs recognizing the N-terminal part of mature FD. The flow-through from this step was tested in two ELISA assays where wells were coated with either of the synthetic peptides. The flow-through preparation was found to be selective for the propeptide only. This Ab pool was termed rabbit anti–pro-FD Ab.

Generation of polyclonal anti–MASP-3 Ab was conducted as described for rabbit anti–pro-FD Ab. The peptide CQMGLPQSVVEPQVER, which corresponds to the very C-terminal part of MASP-3, was used for the immunization. The reactivity of the protein G–purified Ab was verified by ELISA by coating wells with the peptide used for immunization. This Ab pool was termed rabbit anti–MASP-3 Ab.

Time-resolved immunofluorometric assays

Concentrations of MASP-1, MASP-3, and MAp44 in serum samples were measured using previously described sandwich-type immunoassays (43, 44). In all of the assays, detection was achieved using a biotinylated detection Ab followed by addition of Eu^{3+}-labeled streptavidin (1244-360; PerkinElmer, Waltham, MA) diluted to 0.1 μg/ml in TBST (TBS with 0.05% Tween 20), 25 μM EDTA. Protein levels were quantified as the fluorescent signal from Eu^{3+} after addition of 200 μl of enhancement solution (Ampliqon) to each well. Signals were measured as time-resolved fluorometry using a VICTOR X5 plate reader (PerkinElmer) and are given as counts per second.

IEF blots

IEF was performed using the Criterion setup from Bio-Rad, unless otherwise stated. Criterion IEF gels (pH 3–10; 3450071) were placed in a Criterion cell and the lower chamber was filled with anode buffer (7 mM phosphoric acid), whereas the upper chamber was filled with cathode buffer (20 mM lysine, 20 mM arginine). Sample preparation included mixing nine parts of sample with one part of 50% glycerol. An IEF standard ranging from isoelectric points (pIs) 4.45 to 9.6 was used as a marker (161-0310; Bio-Rad). Electrophoresis was conducted in a three-step manner: 100 V for 60 min, 250 V for 60 min, and 500 V for 30 min.

Blotting from the IEF gels is problematic due to the very fragile and sticky nature of the gels. To circumvent this, we used cellulose acetate membranes with a pore size of 0.8 μm (C080A293C; Advantec MFS) as solid support for the gel during the blotting procedure. After focusing, the gel, still resting on the back plate of the cartridge, was soaked for 10 min in 25 mM Tris, 192 mM glycine, 0.1% SDS (pH 8.3) to negatively charge the proteins for the transfer step. The gel was subsequently adhered to a dry cellulose acetate membrane and lifted from the cartridge onto a nitrocellulose membrane (Trans-Blot Turbo Transfer; Bio-Rad). The blotting sandwich was assembled in the following order: anode, gel, cellulose acetate membrane, nitrocellulose membrane, and cathode. Blotting thus occurred through the low protein-binding cellulose membrane and was conducted using the semidry Trans-Blot Turbo Transfer System (Bio-Rad). For higher efficiency, the 7-min transfer protocol supplied by the manufacturer was repeated twice. Residual binding sites on the nitrocellulose membrane were blocked for 1 h at room temperature (RT) in TBST. FD isoforms were detected using a goat anti-FD Ab (AF1824; R&D Systems) diluted to 0.5 μg/ml followed by HRP-labeled rabbit anti-goat Ig Ab (Dako) as the secondary Ab. Detection using the rabbit anti–pro-FD Ab was performed using HRP goat anti-rabbit Ig Ab (Dako) as the secondary Ab. Upon addition of SuperSignal West Pico Chemiluminescent Substrate (Thermo Fisher Scientific), emitted light was detected using a charge-coupled device camera. Pro-FD and FD band intensities were quantified using the software Fiji (45). Note that this approach did not take any nonlinear relationship between protein amount and signal intensity into account.

Analysis of blood samples necessitates removal of some of the most abundant proteins, which was achieved by passing samples through a Vivaspin 500, 100,000 MWCO column (VS0141; Sartorius). After centrifugation at 4°C for 30 min at 15,000 × g, 40 μl of the effluent was loaded onto an IEF gel. In the case of normal plasma or serum, 100 μl of sample was applied to the spin column. For the 3MC samples, of which only small volumes of sample are available, 20 μl of sample is diluted with 180 μl of 0.9% NaCl to minimize sample loss caused by the dead volume of the spin columns (~15 μl). The effluents were subsequently concentrated using Amicon Ultra–0.5 ml 10K spin columns (Merck Millipore) and loaded on a gel. Samples from healthy donors that were used as controls on blots containing 3MC samples were prepared in the same way as the 3MC samples.

Two-dimensional PAGE blots

The samples were dissolved in lysis buffer (7 M urea, 2 M thiourea, 4% [w/v] CHAPS, 10 mM Tris [pH 8.8], 0.5% [v/v] IPG buffer [pH 3–10], and 10 mM DTT) and incubated rotating for 1 h at RT. For each sample, 2 μl of serum was loaded onto 7-cm Immobiline DryStrips (pH 3–10; GE Healthcare Life Sciences). The strips were rehydrated overnight (O/N) at RT, and IEF was performed using the Ettan IPGphor System II (GE Healthcare Life Sciences) for 5.3 kVh. After IEF, proteins were reduced in equilibration buffer (50 mM Tris-HCl [pH 8.8], 6 M urea, 30% [v/v] glycerol, and 2% SDS) with 6.5 mM DTT and then alkylated in equilibration buffer containing 10 mM iodoacetamide. The strips were placed on top of 12.5% SDS-polyacrylamide gels, and the second dimension was run at 17.5 mA per gel in running buffer (25 mM Tris, 192 mM glycine, and 0.1% [w/v] SDS). The proteins were transferred to a nitrocellulose membrane and detected using goat anti-FD, as described for the IEF blots.

Pull-down of pro-FD and FD from NHS

To affinity purify FD isoforms from NHS, we coupled 50 μg of goat anti-FD Ab (AF1824; R&D Systems) to 200 μl of divinyl sulfone-activated Sepharose CL-4B beads. The pull-down was conducted by incubating 200 μl of anti-FD beads with 1 ml of NHS on a rotor O/N at 4°C. The beads were pelleted by centrifugation at 200 × g, 15 min at 4°C, and subsequently washed thrice in TBS. A single additional washing step was performed using TBS, 1 M NaCl, 10 mM EDTA. The FD variants were eluted by applying 1 ml of 0.1 M glycine (pH 2.5). The eluate was dialyzed into TBS and concentrated to ~50 μl using Amicon Ultra–0.5 ml 10K spin columns (Merck Millipore).

Depletion of FD isoforms and MASP-3 from serum

Removal of pro-FD and FD from human serum was conducted as previously described (46). In short, Bio-Rex 70 resin (142-5842; Bio-Rad) was equilibrated in 50 mM NaH_2PO_4, 82 mM NaCl, 2 mM EDTA (pH 7.3). Columns containing 2 ml of resin were used for depleting 0.5 ml of serum containing 10 mM EDTA. Serum-containing fractions were pooled and termed ΔFD serum.

Two milligrams of the Ab 5F5, which recognizes the CCP1 domain of MASP-1/MASP-3/MAp44, were coupled to 2 ml of divinyl sulfone-activated Sepharose CL-4B (43). In parallel, a similar column was prepared with immobilized normal mouse IgG (7404304; Lampire). Up to 5 ml of ΔFD serum was passed over these columns, and serum-containing fractions were pooled to yield ΔFD/ΔMASP-3 from the 5F5 column or ΔFD/Iso from the mouse IgG column. The depletion efficiencies were confirmed by IEF for ΔFD serum and using the MASP-3 immunoassay for ΔFD/Iso and ΔFD/ΔMASP-3. The serum concentration was monitored during the procedure by measuring the total OD280 of the sera.

IEF analysis of pro-FD cleavage in serum

Recombinant pro-FD was added to ΔFD/Iso or ΔFD/ΔMASP-3 serum (22.5%) to a final concentration of 1.82 μg/ml followed by incubation at 37°C. Aliquots (50 μl) were withdrawn at different time points, stopped by adding the protease inhibitor Pefabloc (Sigma) to 2 mM, and analyzed by IEF (described earlier). Similarly, the MASP-3–mediated rescue of conversion in ΔFD/ΔMASP-3 serum was investigated by including MASP-3 WT or S664A at a concentration of 5 μg/ml.

Conversion of endogenous pro-FD in serum was examined by incubating NHS at 37°C for 24 h. Subsequently, the serum was analyzed by IEF blotting. In addition, the effect of exogenous MASP-3 WT or S664A was assessed by adding MASP-3 to a final concentration of 50 μg/ml. This was performed for NHS and serum from patient 3MC #3. The samples were incubated at 37°C for 24 h and analyzed by IEF blotting. Cleavage of affinity-purified FD isoforms from NHS was investigated in a similar manner.

Assay for AP activity on a zymosan surface

The deposition of C3 fragments on a zymosan surface was measured using conditions that block CP and LP activity, as described previously (47). ΔFD/ΔMASP-3 or ΔFD/Iso serum were used at a final concentration of 13.3% in VBS/EGTA/Mg^{2+} buffer (5 mM barbital, 145 mM NaCl, 10 mM EGTA, 25 mM $MgCl_2$ [pH 7.4]). Recombinant pro-FD was added to a concentration of 0.35 μg/ml together with buffer or recombinant MASP-3 WT or S664A. The samples were incubated for 2 h at 37°C before transferring

40 μl to zymosan-coated microtiter wells. The plate was incubated for 1.5 h at 37°C, washed with TBST, and C3 deposition was estimated using 0.5 μg/ml biotinylated rabbit anti-C3d (A0063; Dako) followed by streptavidin-Eu^{3+} addition (see *Time-resolved immunofluorometric assays*). The signal from ΔFD/Iso serum without recombinant MASP-3 was defined as 100% and used to normalize the data. The ability of MASP-3 mutants to rescue AP activity in ΔFD/ΔMASP-3 serum was examined by adding MASP-3 culture supernatant to a final MASP-3 concentration of 9.2 μg/ml.

Assay for AP activity using hemolysis

The hemolysis assay was performed with minor modifications to a previously published method (36). Samples consisting of 20% depleted sera and 0.12 μg/ml recombinant pro-FD were prepared in VBS/EGTA/Mg^{2+} buffer with 0.1% gelatin. In some cases, varying concentrations of MASP-3 WT or S664A were likewise included. These samples were preincubated for 2 h at 37°C before transferring 20 μl to rabbit erythrocytes (Statens Serum Institut). Lysis was achieved by 2 additional hours of incubation at 37°C and was estimated as the absorbance at 405 nm. A water sample was included to yield maximal lysis, and the resulting A405 was defined as 100% for each plate.

In vivo studies using Masp1/3$^{-/-}$ mice

Animals were housed in type II plastic cages (Techniplast) in a temperature-controlled pathogen-free animal facility, with unrestricted access to diet (1324; Altromin, Lage, Germany) and tap water. The animal room had a 12:12 h light/dark cycle (lights on at 6:00 AM). The experiments were approved by the Danish Experimental Inspectorate (J.no. 2014-15-0201-00377), and housing of the mice was carried out according to Danish legislation and the Directive 2010/63/ on the protection of animals used for scientific purposes.

Recombinant MASP-3 (50 μg of recombinant MASP-3 per 20 ng mouse) was administered by i.v. tail injection into male C57BL/6 Masp1/3$^{-/-}$ mice, kindly donated by the late M. Takahashi (32), in a volume of 400 μl. EDTA plasma was withdrawn from the facial vein at times 0 h, 4 h, 24 h, 1 wk, and 2 wk after injection (~50 μl). The AP activity was estimated by rabbit erythrocyte lysis, as described earlier with few modifications. The plasma was diluted to 8.33% in 5 mM barbital, 145 mM NaCl, 10 mM EGTA, 10 mM MgCl$_2$ [pH 7.4], and the microtiter plate containing erythrocytes mixed with plasma was incubated at 37°C for 3.5 h before measuring the absorbance at 405 nm.

Pro-FD conversion assay

To establish an assay that monitors the removal of the propeptide from pro-FD, we biotinylated recombinant pro-FD using biotin *N*-hydroxysuccinimide ester (Sigma), as previously described (43). Microtiter wells were coated with 2 μg/ml rabbit anti–pro-FD (described earlier) diluted in PBS by O/N incubation at RT. Residual binding sites were blocked by incubation with 1 mg/ml HSA in TBS for 1 h at RT. The wells were washed thrice with TBST between each step of the assay. Samples of 100 μl with 150 ng/ml biotinylated pro-FD were added to each well and incubated for 1 h at RT. Detection of bound pro-FD was performed using streptavidin-Eu^{3+}, as described earlier. The signals were quantified by including a standard of biotinylated pro-FD starting at 600 ng/ml with 10 subsequent 2-fold dilutions.

To examine the MASP-3–mediated conversion of pro-FD, we prepared samples containing 9.6 μg/ml biotinylated pro-FD in TBS and 17 or 1.7 μg/ml recombinant MASP-3. Alternatively, culture supernatant was added to yield a MASP-3 concentration of 100 μg/ml for investigating the enzymatic capability of different MASP-3 mutants. Conversion of pro-FD in depleted sera was investigated by concentrating the sera to 100% (based on total protein content) using Amicon Ultra–0.5 ml 10K spin columns (Merck Millipore). Subsequently, biotinylated pro-FD was added to a final concentration of 8.6 μg/ml, resulting in a final serum concentration of 86%. In all cases, samples were incubated at 37°C and aliquots were withdrawn at different time points. The conversion was stopped by addition of Pefabloc to 1 mM, and the remaining noncleaved biotinylated pro-FD was estimated as described earlier.

The estimation of the time required for converting 50% of the pro-FD substrate (conv$_{1/2}$) of biotinylated pro-FD in pools of either serum or EDTA plasma from 10 healthy donors was performed by mixing 80 μl of blood sample with 4 μl of biotinylated pro-FD, yielding 95.2% NHS or EDTA plasma. Aliquots were withdrawn and analyzed as described earlier. The conv$_{1/2}$ was estimated assuming that the conversion followed first-order kinetics, and analysis was performed by fitting the data to the standard one-phase decay equation in Prism v.6 (GraphPad Software, La Jolla, CA).

Analysis of circulating MASP-3

One milligram of rabbit anti–MASP-3 Ab was coupled to 1 ml of divinyl sulfone-activated Sepharose CL-4B, and in parallel similar beads were prepared with immobilized normal rabbit IgG (7406404; Lampire). All of the following steps were performed at 4°C. A pool of EDTA plasma from 30 healthy donors was prepared, and Pefabloc was added to a final concentration of 5 mM. One milliliter of the plasma pool was passed over either the anti–MASP-3 beads or the rabbit IgG beads. Subsequently, unbound proteins were washed away using 15 ml of TBS, 5 mM EDTA, and 2 mM Pefabloc. Bound MASP-3 was eluted in 0.5 ml fractions by adding 0.1 M glycine (pH 2.5), and the fractions were neutralized by mixing with 1 M Tris (pH 8.5). MASP-3–containing fractions were identified using the MASP-3 time-resolved immunofluorometric assay and were pooled. The corresponding fractions from the rabbit IgG column were likewise pooled. Pefabloc was added to the pools to a final concentration of 2 mM, and the eluates were concentrated using Amicon Ultra–0.5 ml 10K spin columns (Merck Millipore). The eluates were then analyzed by Western blotting using the rabbit anti–MASP-3 Ab as the primary Ab. The ratio between zymogenic and activated MASP-3 was quantified by densitometry using the software Fiji (45).

Assay for MASP-3 binding to MBL

Microtiter wells were coated with 100 μl of 1 μg/ml recombinant MBL in PBS at RT. Subsequently, wells were blocked with 1 mg/ml HSA diluted in TBS. The wells were washed thrice with TBST, 5 mM CaCl$_2$ between each step of the assay. The MASP-3–containing culture supernatants were diluted in TBST, 5 mM CaCl$_2$, and 1 mg/ml HSA to yield MASP-3 concentrations of 5, 0.5, or 0.05 μg/ml, and 100 μl was added to each MBL-coated well. The plate was incubated for 1.5 h at RT followed by addition of 0.5 μg/ml biotinylated anti–MASP-3 Ab (5F5). After 2 h of incubation at RT, detection was achieved using streptavidin-Eu^{3+}. MASP-3 WT diluted in TBST, 1 M NaCl, and 10 mM EDTA was included as a negative control. The buffer background was subtracted from the signals, and the signal from the sample containing 5 μg/ml MASP-3 WT was defined as 100% binding.

Statistical analyses

All graphs and statistical analyses were performed using GraphPad Prism version 6 (GraphPad Software). Data are shown as means, and error bars represent SD.

Results

The MASP-3 G665S mutation causes 3MC syndrome

A proposita was identified with clinical features suggesting 3MC syndrome. Sanger sequencing revealed that the patient was homozygous for a novel missense mutation c.1993G>A (p.G665S) in exon 12 of *MASP1*, confirming the clinical diagnosis of 3MC syndrome. Residue 665 is located within a mutational hotspot next to the previously described 3MC mutations p.D663Y and p.G666E (37). The concentration of MASP-3 in serum from this patient (3MC #1) was 3.7 μg/ml, which is lower than the median level in a healthy population [6.68 μg/ml with an interquartile range of 5.56–8.30 μg/ml (44)]. In contrast, the concentrations of the other *MASP1* splice products MASP-1 and MAp44 were within the interquartile range of healthy donors (data not shown).

Analysis of endogenous pro-FD and mature FD by IEF blotting

To investigate the ratio between pro-FD and FD in serum from patient 3MC #1, we had to develop a method that enables analytical separation of the endogenous FD variants in complex samples. This is complicated by the fact that pro-FD and FD vary by only 6 aa. Because the propeptide contains two arginine residues, we developed a technique based on IEF that separates proteins according to their pI. Upon electrophoretic separation, the proteins were transferred to a membrane and detected with an Ab that recognized both pro-FD and FD. This resulted in clear separation of the purified FD isoforms, corresponding well to a theoretical pI difference of one full unit between the isoforms (Fig. 1A, top). Furthermore, IEF blotting was analytically superior to standard Western blotting, which yielded inadequate separation

of the proteins (Fig. 1A, bottom). An SDS-PAGE gel of the purified proteins used throughout the present study is shown in Supplemental Fig. 1.

The analysis of the pro-FD/FD ratio in blood samples required a preparation step, because focusing in our setup was incompatible with the high protein concentration in serum and plasma. By passing the sample through a spin column with an appropriate molecular weight cutoff, pro-FD and FD were collected in the effluent, whereas abundant larger proteins, such as albumin and Igs, were retained by the membrane. Subsequently, the FD isoforms were readily resolved by IEF blotting. To verify the technique, we first analyzed NHS before and after FD depletion using Bio-Rex 70 resin. Bands corresponding to pro-FD and FD were present in the starting material, whereas no apparent bands were seen after depletion (Fig. 1B, left). A similar result was obtained when analyzing a commercially available FD-depleted serum, thus further confirming that the bands were indeed FD variants.

Serum from the novel 3MC #1 patient was analyzed together with sera from the previously described patients 3MC #2 and #3, which harbor mutations that lead to nondetectable levels of MASP-3 (28, 37). The distribution of FD variants was found to be heavily biased toward the proenzymatic form in all of the patients. Noticeably, a small level of mature FD was also observed in these samples (Fig. 1B, right). Aside from the bands corresponding to pro-FD and FD, a less intense band with a slightly larger pI value than FD was detected. The nature of this FD variant is currently unknown. NHS and 3MC serum were also examined using two-dimensional SDS-PAGE and subsequent blotting. These results supported the observations from the IEF analysis, because the two-dimensional blot of NHS yielded two spots corresponding to pro-FD and FD, whereas the pro-FD spot was dominant in the 3MC serum (Fig. 1C). Moreover, two-dimensional blots of other sera displayed similar pro-FD/FD ratios as those observed using IEF, thus further verifying the results (data not shown).

Plasma samples were likewise applicable to IEF blotting, although serum generally gave stronger signals, most likely because of the loss of coagulation factors (and other proteins) during clotting (Supplemental Fig. 2). EDTA plasma from patient 3MC #3 was analyzed to assess whether the mature FD observed in serum from this patient was generated as a result of the clotting process, and it was found that mature FD was also detectable in 3MC plasma (Supplemental Fig. 2).

FIGURE 1. The pro-FD/FD ratio in 3MC patients. (**A**, top) IEF analysis of purified pro-FD and FD. FD displays an approximate pI of 7.2, which is in accordance with the theoretical value, whereas the pI value of pro-FD is estimated to be around 8. The IEF blot contains 25, 50, or 100 ng of FD or pro-FD from left to right. Bottom, The Western blot excerpt highlights the poor separation of pro-FD and FD achieved with this technique. A total of 25, 50, 100, or 200 ng of FD or pro-FD was loaded from left to right. Note that the Ab displays comparable affinities toward pro-FD and FD. These blots are representative of three experiments. (**B**, left) IEF analysis of control sera. The left lane shows NHS #2, the ΔFD lane is NHS #2 after depletion of FD isoforms, and ΔFD (CT) is FD-depleted serum from Complement Technology (Tyler, TX). Right, IEF blotting of serum samples from 3MC patients. Patient 3MC #1 is the patient presented in this study, whereas 3MC #2 and #3 are described in detail elsewhere (see *Materials and Methods*). The low signal intensity seen for 3MC #1 is due to an inherent low total pro-FD/FD level in the sample, as verified by Western blotting (data not shown). An NHS control is included, and the positions of pro-FD and FD are indicated by arrows. The left blot is representative of three experiments, whereas the right blot was conducted only once because of the scarcity of the 3MC samples. (**C**) Two-dimensional blots of NHS #3 (left) and 3MC #2 (right) reproduce the result observed in (B). Horizontally, serum proteins were focused between a pH gradient from 3 to 10. In the vertical direction, proteins were separated according to size using SDS-PAGE. The blot of NHS is representative of three different sera, whereas the 3MC blot is representative for both 3MC #2 and #3.
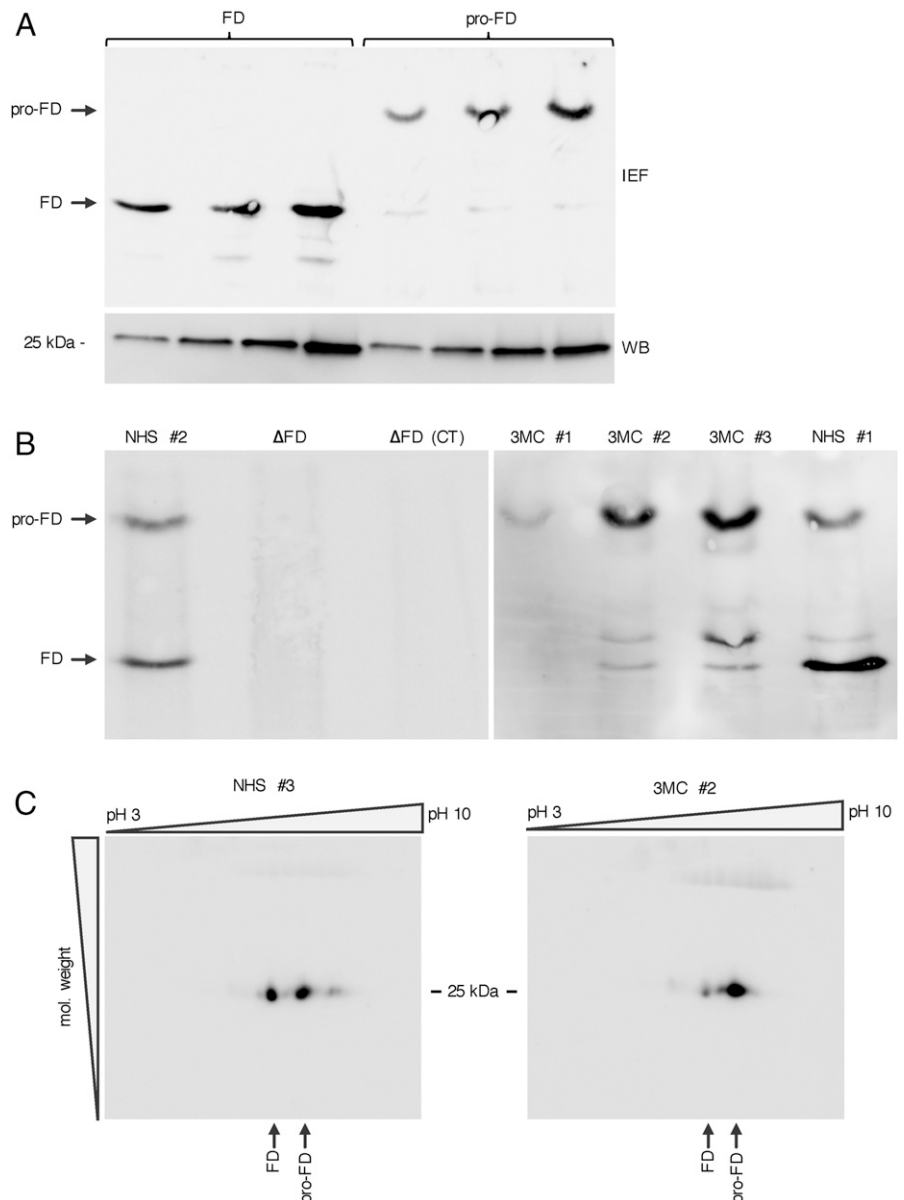
Pro-FD exists in the circulation of healthy individuals

A striking result from the experiments presented in Fig. 1 was the identification of pro-FD in blood samples from healthy donors (Fig. 1B, 1C). This encouraged us to analyze NHS from 18 different donors, which showed that circulating pro-FD was present in all of these individuals (Fig. 2A, Supplemental Fig. 3). The ratio between FD and pro-FD in the sera was estimated using densitometry and was found to vary considerably, ranging from a large excess of mature FD to comparable amounts of the two variants. Furthermore, the ratio seemed to be stable for a given individual, because blood samples drawn at different times displayed comparable ratios (data not shown). To further confirm the nature of the pro-FD band, we developed a polyclonal Ab that specifically recognized pro-FD but did not react with FD. Using this Ab in IEF blotting, the position of endogenous pro-FD was shown to exactly match that of recombinant pro-FD (Fig. 2B). In addition, no signal was seen in the control lane containing only mature FD. The identities of bands other than those corresponding to pro-FD and FD are unknown (Fig. 2A, 2B).

Next, we investigated whether the endogenous pro-FD was readily converted into mature FD. The pro-FD content of NHS was not affected by 24 h of incubation at 37°C before IEF analysis.

Moreover, pro-FD conversion was not induced by addition of recombinant MASP-3 to the serum (Fig. 2C). To ensure that the serum possessed the ability to cleave pro-FD, we added a surplus of recombinant pro-FD, and this was found to be converted into FD (data not shown). The nonconvertible nature of endogenous pro-FD persisted when pro-FD and FD were affinity purified from NHS and incubated with recombinant MASP-3, whereas recombinant pro-FD that was purified using the same strategy was converted into FD (Fig. 2C). In contrast with NHS, the pro-FD in 3MC serum was converted into FD when exogenous MASP-3 was supplied (Fig. 2C).

Lack of MASP-3 impacts the conversion of pro-FD to FD

To create a platform that allowed extensive examination of the MASP-3–driven maturation of pro-FD, we sequentially depleted serum of pro-FD/FD and MASP-3. The first depletion step was efficient, because no bands were seen when the resulting ΔFD serum was analyzed by IEF blotting (Fig. 1B). Subsequently, ΔFD serum was either depleted of MASP-3, creating ΔFD/ΔMASP-3, or passed over a column of an isotype control Ab, resulting in ΔFD/Iso serum. MASP-3 was undetectable in ΔFD/ΔMASP-3, indicating a concentration <50 ng/ml, whereas the concentration
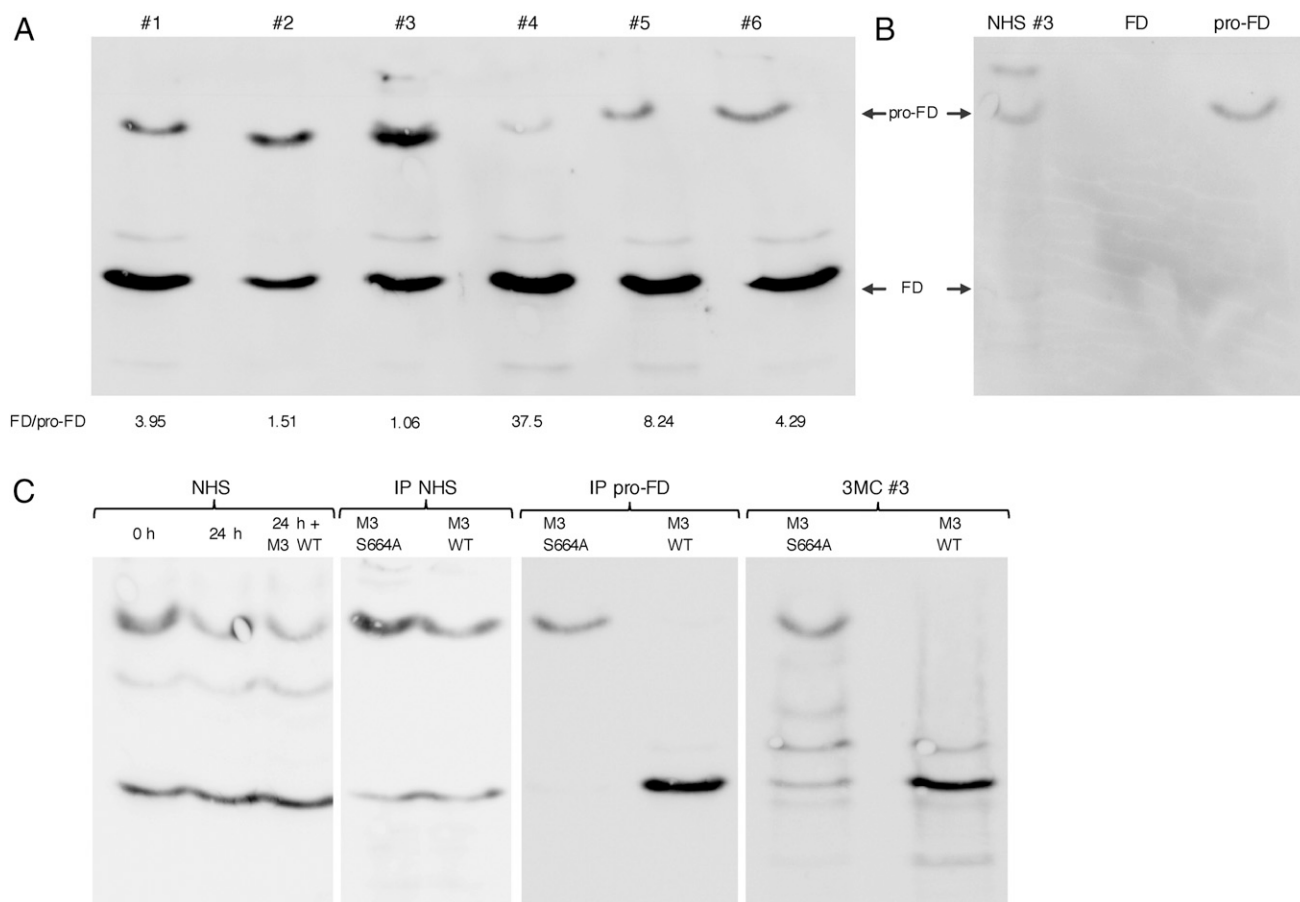

FIGURE 2. Identification of pro-FD in the circulation of healthy donors. (**A**) IEF blot of NHS from six different donors. The ratio between the band intensities for FD and pro-FD in a given serum was quantified using densitometry and is shown below each lane (FD/pro-FD). All samples were analyzed at least twice with similar results; however, the FD/pro-FD ratio was based on the depicted blot. (**B**) Detection of pro-FD using anti–pro-FD Ab. An IEF blot of NHS #3 is developed with an Ab that specifically recognizes pro-FD and not FD. As controls, 5 ng of purified FD or pro-FD was included. This was repeated twice for NHS #3 and twice for NHS #2 with similar results (data not shown). (**C**) Endogenous pro-FD was not converted into FD in NHS. The left blot shows NHS that was incubated at 37°C and analyzed by IEF blotting. MASP-3 was added to the rightmost lane to a concentration of 50 μg/ml. In the two middle blots, pro-FD was purified by immunoprecipitation (IP). Subsequently, the sample was mixed with MASP-3 WT or S664A and incubated for 24 h at 37°C before IEF analysis. The IP was performed from NHS (IP NHS) or using recombinant pro-FD (IP pro-FD) as a control to ensure that the elution step (pH 2.5) did not damage pro-FD. The rightmost blot depicts serum from 3MC #3, which has been incubated for 24 h at 37°C with 50 μg/ml inactive (M3 S664A) or active (M3 WT) MASP-3. These experiments were repeated twice, except for the blot including the 3MC sample, which was performed only once because of lack of material.

in ΔFD/Iso was unaffected by the treatment (data not shown). MASP-1 and MAp44 were also removed from ΔFD/ΔMASP-3, because the Ab used for MASP-3 depletion recognized the CCP1 domain, which is shared by the three *MASP1*-encoded proteins. ΔFD/ΔMASP-3 serum thus mimics the state found in a subset of 3MC patients and in *Masp1/3*[−/−] mice, where all three splice variants are absent.

The ability of the depleted sera to cleave pro-FD was examined by adding purified pro-FD and following the kinetics of conversion by IEF (Fig. 3A, left). ΔFD/Iso serum readily converted pro-FD with a FD band appearing after 1 h that steadily increased in intensity with time. In contrast, there was very little conversion in ΔFD/ΔMASP-3, with only a minor level of background conversion after 8 h. An unidentified band with a pI value between those of pro-FD and FD appeared with the same rate as FD. Furthermore, the pro-FD–cleaving ability of ΔFD/ΔMASP-3 could be rescued by addition of MASP-3 WT, whereas the inactive MASP-3 S664A control did not have any effect (Fig. 3A, right). To investigate whether pro-FD cleavage translated into AP activity, we measured C3 fragment deposition by the AP on an activating zymosan surface. The ΔFD/Iso serum readily deposited C3 on the surface, whereas ΔFD/ΔMASP-3 resulted in deposition levels close to the background. This difference was gradually decreased as the sera were reconstituted with MASP-3 (Fig. 3B). Similar results were obtained using an assay that measured the ability of the AP to lyse

rabbit erythrocytes, thus reflecting not only C3 deposition, but also the terminal part of the complement system (Fig. 3C).

To further consolidate the necessity of MASP-3 for a fully active AP, we used *Masp1/3*[−/−] mice as an in vivo model for indirect assessment of pro-FD maturation. This was conducted by measuring the MASP-3–mediated rescue of AP activity, which is known to be compromised in these mice (32). Purified murine MASP-3 was injected into the mice, and EDTA plasma withdrawn at different time points was tested for its ability to lyse rabbit erythrocytes through the AP. Active MASP-3 dramatically enhanced the AP activity compared with the low level of lysis seen in the control mice that received the inactive S669A variant (Fig. 4). At 4 and 24 h after injection of MASP-3 WT, the plasma was capable of lysing the erythrocytes to the same extent as EDTA plasma from normal C57BL/6 mice. The AP activity had returned to the baseline level a week after injection.

Examination of pro-FD conversion by an immunoassay

To quantify the conversion of pro-FD into FD, we developed an assay that relies on the pro-FD–specific Ab introduced in Fig. 2B. Microtiter wells were coated with anti–pro-FD Ab, and samples containing biotinylated pro-FD were subsequently added. Using europium-labeled streptavidin, we exploited the biotin–streptavidin interaction for detection, because the fluorescent signal correlated with the amount of bound biotinylated pro-FD. Thus, the
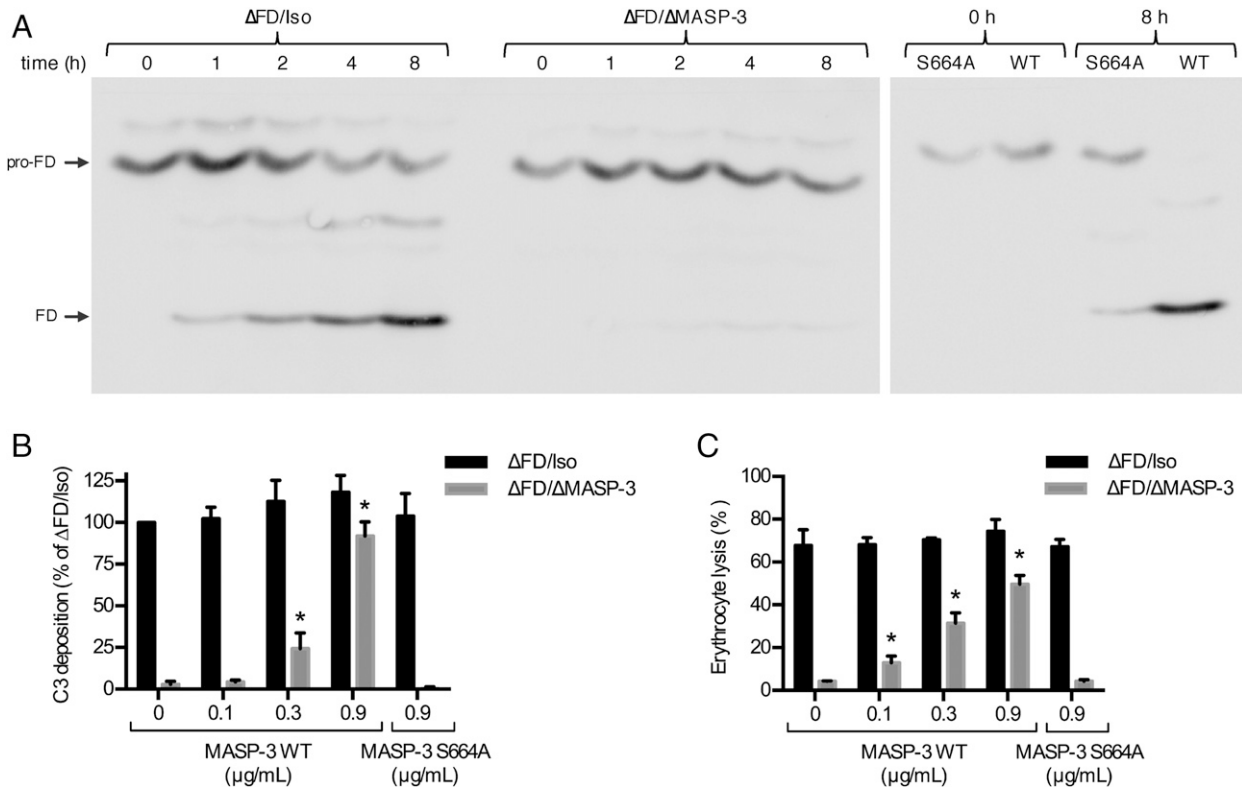

FIGURE 3. Pro-FD cleavage is drastically reduced in MASP-3–depleted serum. (**A**) Conversion of pro-FD in depleted sera. Pro-FD was added to a final concentration of 1.8 μg/ml to ΔFD/ΔMASP-3 or ΔFD/Iso serum and incubated at 37°C. Left, Aliquots were withdrawn at the indicated time points and analyzed using IEF. Right, Pro-FD and MASP-3 WT or S664A were added to ΔFD/ΔMASP-3 serum and incubated for 8 h before IEF analysis. Both blots are representative of three experiments. (**B**) AP activity in depleted sera was estimated as C3 deposition on a zymosan-coated surface. Pro-FD was added to depleted sera to a final concentration of 0.35 μg/ml together with varying concentrations of MASP-3 WT or S664A, as indicated. The activity of ΔFD/Iso serum without exogenous MASP-3 was defined as 100% and used for normalizing the data. Within the ΔFD/Iso and the ΔFD/ΔMASP-3 groups, C3 deposition levels were compared with the sample without added MASP-3 by an unpaired parametric t test. *p < 0.02 (n = 3). (**C**) The ability of depleted sera to lyse rabbit erythrocytes was used as a measure for AP activity. Pro-FD was added to depleted serum together with varying concentrations of MASP-3, and lysis was estimated by measuring the absorbance at 405 nm. Osmotic lysis of erythrocytes using water yielded the maximal level of lysis and was defined as 100%. For each serum, the percentage of lysis for samples containing recombinant MASP-3 was compared with the sample without MASP-3 addition using an unpaired parametric t test. *p < 0.01 (n = 3).
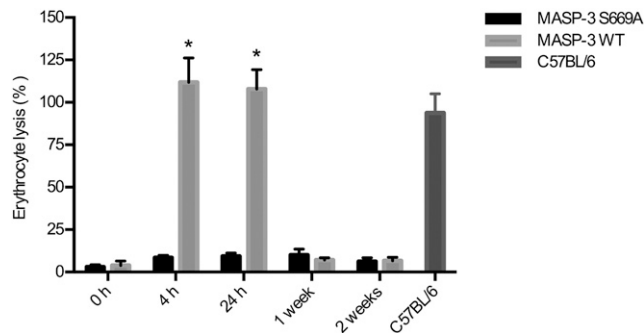
FIGURE 4. Rescue of AP activity by MASP-3 in *Masp1/3*$^{-/-}$ mice. Purified murine MASP-3 WT or the inactive S669A mutant was injected i.v. into male *Masp1/3*$^{-/-}$ mice. EDTA plasma was withdrawn at the indicated time points, and the AP activity was quantified as the ability to lyse rabbit erythrocytes. As a reference, the AP activity of noninjected C57BL/6 mice is included. Osmotic lysis of erythrocytes using water yielded the maximal level of lysis and was defined as 100%. The level of lysis was compared for each time point using an unpaired parametric *t* test. *$p <$ 0.0001 (*n* = 5).

assay was expected to show a decreasing signal as pro-FD was converted into FD in a given sample. However, this expectation strictly relied on the ability of anti–pro-FD to discriminate between pro-FD and FD. This was investigated using samples containing a constant concentration of biotinylated pro-FD together with varying concentrations of unlabeled pro-FD or FD to compete for Ab binding. The signal was gradually inhibited by the addition of pro-FD, whereas no significant effect was seen for mature FD (Fig. 5A). Hence, our assay enabled the MASP-3–mediated cleavage of pro-FD to be followed in a purified system. A pronounced decrease in signal was seen when biotinylated pro-FD was incubated with MASP-3 WT, whereas no cleavage was observed for the inactive S664A mutant (Fig. 5B). Furthermore, the conversion displayed a clear dependency on the concentration of MASP-3.

There have been opposing reports regarding whether zymogenic MASP-3 possesses pro-FD–cleaving activity (33, 34). Therefore, we produced the zymogenic MASP-3 R449Q variant, which was not activated because of the mutation in its activation site that prevents cleavage by trypsin-like proteases. The zymogenic nature of this MASP-3 variant was assessed by SDS-PAGE under reducing conditions. In contrast with MASP-3 WT and MASP-3 S664A, there are no detectable bands corresponding to activated A and B chains for MASP-3 R449Q (Supplemental Fig. 1). This zymogenic mutant was found to lack enzymatic activity, because no statistically significant cleavage was observed even after 24 h of incubation with pro-FD (Fig. 5B). Because this result implied that activated MASP-3 must be present in the circulation, the degree to which circulating MASP-3 is activated was examined. MASP-3 was affinity purified from a Pefabloc-containing pool of EDTA plasma from healthy donors and was analyzed using Western blotting. It was found that a portion of MASP-3 is indeed present as an activated enzyme, because ~40% was found to be activated (Supplemental Fig. 4).

The immunoassay also permitted pro-FD maturation to be monitored in a complex matrix, meaning that the difference in conversion capability between ΔFD/Iso and ΔFD/ΔMASP-3 serum could be quantified. Again, we observed a clear difference in the pro-FD–cleaving kinetics of the sera. In ΔFD/Iso serum, roughly 45% of the biotinylated pro-FD was cleaved after 2 h, with complete conversion being reached after 24 h. In contrast, 24 h of incubation was necessary to observe statistically significant conversion in ΔFD/ΔMASP-3 serum (Fig. 5C). To study the kinetics of pro-FD maturation in more detail, we investigated the conversion of biotinylated pro-FD in NHS and in EDTA plasma. The conversion of pro-FD was

well described by an exponential decay function, yielding a conv$_{1/2}$ (the time at which half of the initial biotinylated pro-FD is converted) of 2.6 h for NHS and 3.3 h for EDTA plasma (Fig. 5D).

MASP-3 variants found in 3MC patients are enzymatically inactive

As described earlier, we found that serum from patient 3MC #1 predominantly contained pro-FD, despite the substantial level of circulating MASP-3. To investigate the mechanistic link between these observations, and to further stress the role of MASP-3 in pro-FD maturation, we characterized the functional effects of the nine distinct MASP-3 mutations identified in 3MC patients. HEK293 cells were transfected with plasmids encoding the known variants to investigate the effect on the MASP-3 expression levels. The expression was quantified by measuring the concentration of MASP-3 in the culture supernatant using an MASP-3–specific immunoassay. The results were confirmed by Western blot analysis, because the mutations could potentially influence the binding to the Abs used in the assay. All mutations except G687R were found to decrease the expression level to <25% of the WT level (Fig. 6A), whereas three of the mutations prevented MASP-3 expression entirely.

The level of binding to MBL was assessed as a measure of the ability of the proteins to bind to PRMs, and all expressing mutants displayed WT-like binding properties (Fig. 6B). We investigated whether the MASP-3 mutants could cleave biotinylated pro-FD, because none of the MASP-3 mutants have been characterized enzymatically against a biologically relevant substrate. MASP-3 WT fully converted pro-FD into FD, whereas none of the mutants cleaved the substrate (Fig. 6C). The lack of enzymatic activity of the mutants was further verified by adding the MASP-3 variants to ΔFD/ΔMASP-3 serum together with pro-FD and measuring the resulting AP-mediated C3 deposition. This confirmed the inactive nature of the 3MC-causing mutants, because only MASP-3 WT was capable of inducing C3 fragment deposition (Fig. 6D).

Discussion

Since the original report of circulating pro-FD in *Masp1/3*$^{-/-}$ mice, the role of MASP-1 and MASP-3 in the AP of complement has been widely debated. It is now evident that MASP-3, and not MASP-1, is involved in cleaving pro-FD into FD (33–35). However, the strict dependence of the AP on the MASP-3–mediated cleavage of pro-FD has remained controversial. With the aim of resolving this issue, we have developed tools to analytically investigate the FD variant distribution and the cleavage of pro-FD in complex samples.

We present a novel analytical method that yields good separation of FD and pro-FD by exploiting the basic nature of the FD propeptide, which contains two arginine residues. Previously, traditional Western blotting has been used to distinguish between pro-FD and FD in blood samples, based on a slight band shift caused by the removal of 6 aa. Although this approach has provided qualitatively sound results (32, 33, 38, 48), we find that the poor resolution tends to result in an all-or-nothing interpretation, thereby masking important nuances regarding the pro-FD/FD relationship (39). One study circumvented this issue by using cation exchange chromatography to separate the isoforms and quantify the ratio between them (34). However, this strategy is only applicable to the analysis of pro-FD conversion in highly purified systems. An alternative method uses Cy3-labeled pro-FD combined with in-gel fluorescence to follow pro-FD conversion in blood samples (34, 35). Although this does allow investigation of the cleavage of exogenous pro-FD in complex samples, it does not enable detection of endogenous FD isoforms and their interrelationship. We show that our IEF blotting setup transcends these limitations,
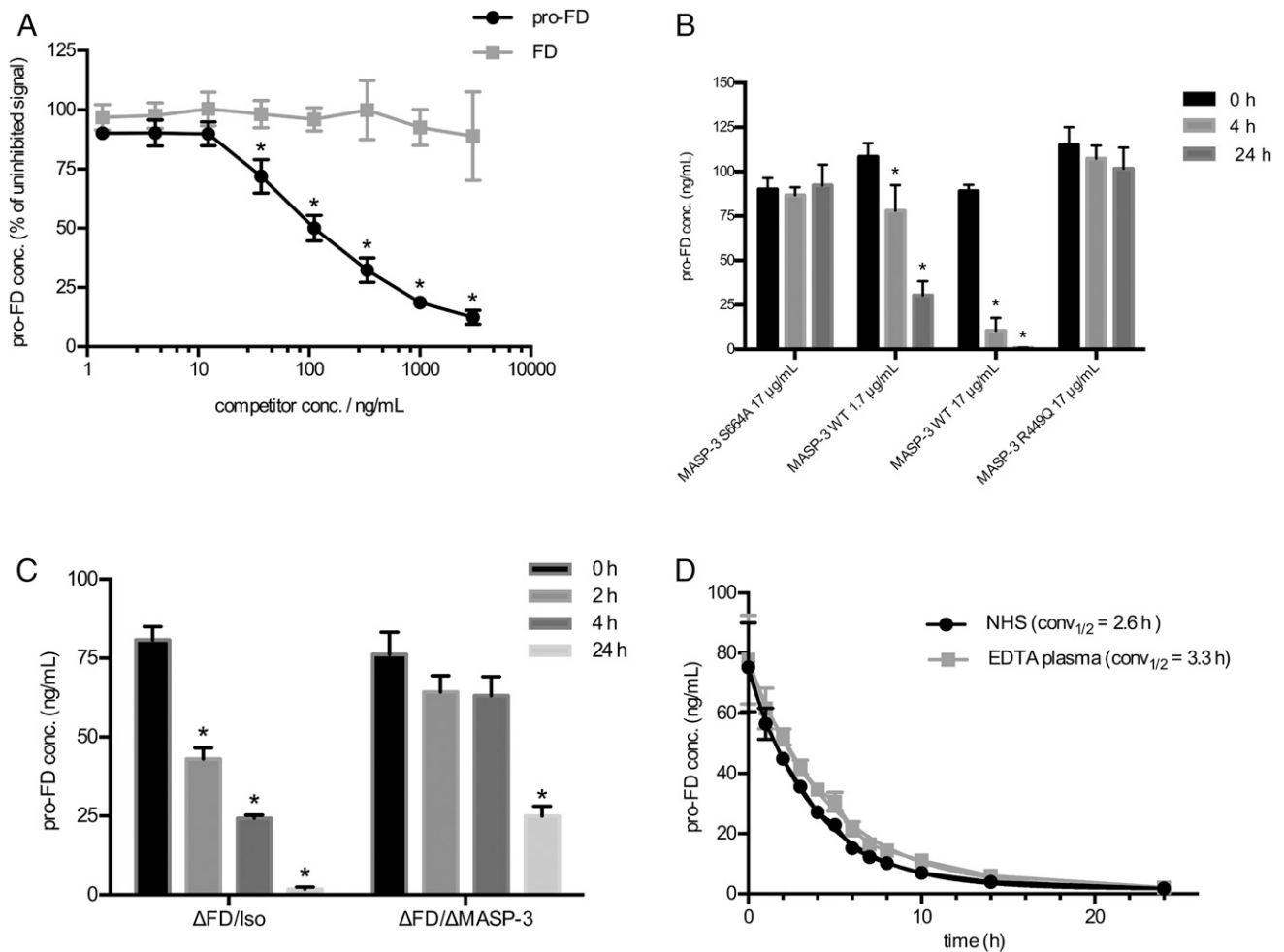
FIGURE 5. An immunoassay to monitor the conversion of pro-FD to FD. (**A**) Assay specificity. Varying concentrations of pro-FD or FD were added together with 150 ng/ml biotinylated pro-FD to follow the competition between the labeled and unlabeled proteins. Samples without unlabeled competitor were used for normalization and assigned 100% signal. The signals at a given competitor concentration were compared by an unpaired parametric t test. $*p < 0.01$ ($n = 3$). (**B**) Conversion of pro-FD by purified MASP-3. Biotinylated pro-FD was incubated at 37°C with 17 or 1.7 µg/ml MASP-3 WT, 17 µg/ml MASP-3 S664A, or 17 µg/ml MASP-3 R449Q, and cleavage was stopped after 0, 4, and 24 h. Subsequently, the amount of pro-FD left in the sample was measured. Within each group, the pro-FD concentrations at 4 and 24 h were compared with the starting value using an unpaired parametric t test. $*p < 0.05$ ($n = 3$). (**C**) Pro-FD conversion in depleted sera. Biotinylated pro-FD was added to ΔFD/Iso or ΔFD/ΔMASP-3 serum and incubated at 37°C. Samples were withdrawn at the indicated time points, and the amount of remaining pro-FD in the sample was measured. For each serum, the pro-FD concentrations at 2, 4, and 24 h were compared with the starting value using an unpaired parametric t test. $*p < 0.0003$ ($n = 3$). (**D**) Quantification of pro-FD conversion kinetics in blood samples. A final mixture of NHS or EDTA plasma (95%) and biotinylated pro-FD was incubated at 37°C, and samples were withdrawn and stopped at the indicated time points ($n = 3$). The $conv_{1/2}$, which is the time it takes for converting half of the biotin pro-FD, was estimated by fitting the data to an exponential decay function ($r^2_{NHS} = 0.97$, $r^2_{EDTA} = 0.97$). The 95% confidence intervals of the $conv_{1/2}$ were determined as 2.24–3.02 h for NHS and 2.74–3.82 h for EDTA plasma. Note that the concentrations on the y-axis in (B)–(D) are the concentrations in the samples after aliquots were withdrawn and diluted. During the conversion step, the pro-FD concentration was 8.6 µg/ml.

because both the endogenous pro-FD/FD ratio and the conversion of exogenous pro-FD are easily monitored (Figs. 1–3).

Using IEF blotting, we were able to examine serum from 3MC patients, including a sample from a previously undescribed patient carrying the novel G665S mutation. 3MC samples are unique matrices for investigating the biological role of MASP-3, but as mentioned earlier, they have been a source of seemingly opposing observations in the literature. AP activity was found to be reduced but present in the sera from patients 3MC #2 and #3, despite their MASP-3 deficiency (36, 37). Western blot analysis of the same sera, however, showed that they solely contained pro-FD (39). This discrepancy was further augmented when similarly inconclusive results were generated using $Masp1/3^{-/-}$ mice, where the activity of the AP in serum was dependent on the type of buffer system used in the assay (49). In this article, we showed that although the majority of FD in the 3MC samples was indeed found

in the proenzymatic state, the sera nonetheless contained detectable levels of mature FD (Fig. 1B). Our results thus unify the conflicting observations in the literature, by highlighting that although MASP-3 does appear to be the main converter of pro-FD, a lower level of mature FD is still generated in sera lacking MASP-3 activity. Using an MASP-3–specific inhibitor, a previous study reported that MASP-3 inhibition completely abolished pro-FD cleavage in plasma, whereas residual activity persisted in serum (35). It was therefore hypothesized that proteases that are activated during clotting, such as those from the coagulation system, act as backup enzymes that can cleave pro-FD. Moreover, this led to the suggestion that the AP activity observed in 3MC samples might be a serum-specific feature that is not necessarily representative of the in vivo scenario (35). However, we show that mature FD was also detected in EDTA plasma from a 3MC patient, indicating that the residual pro-FD–cleaving activity may
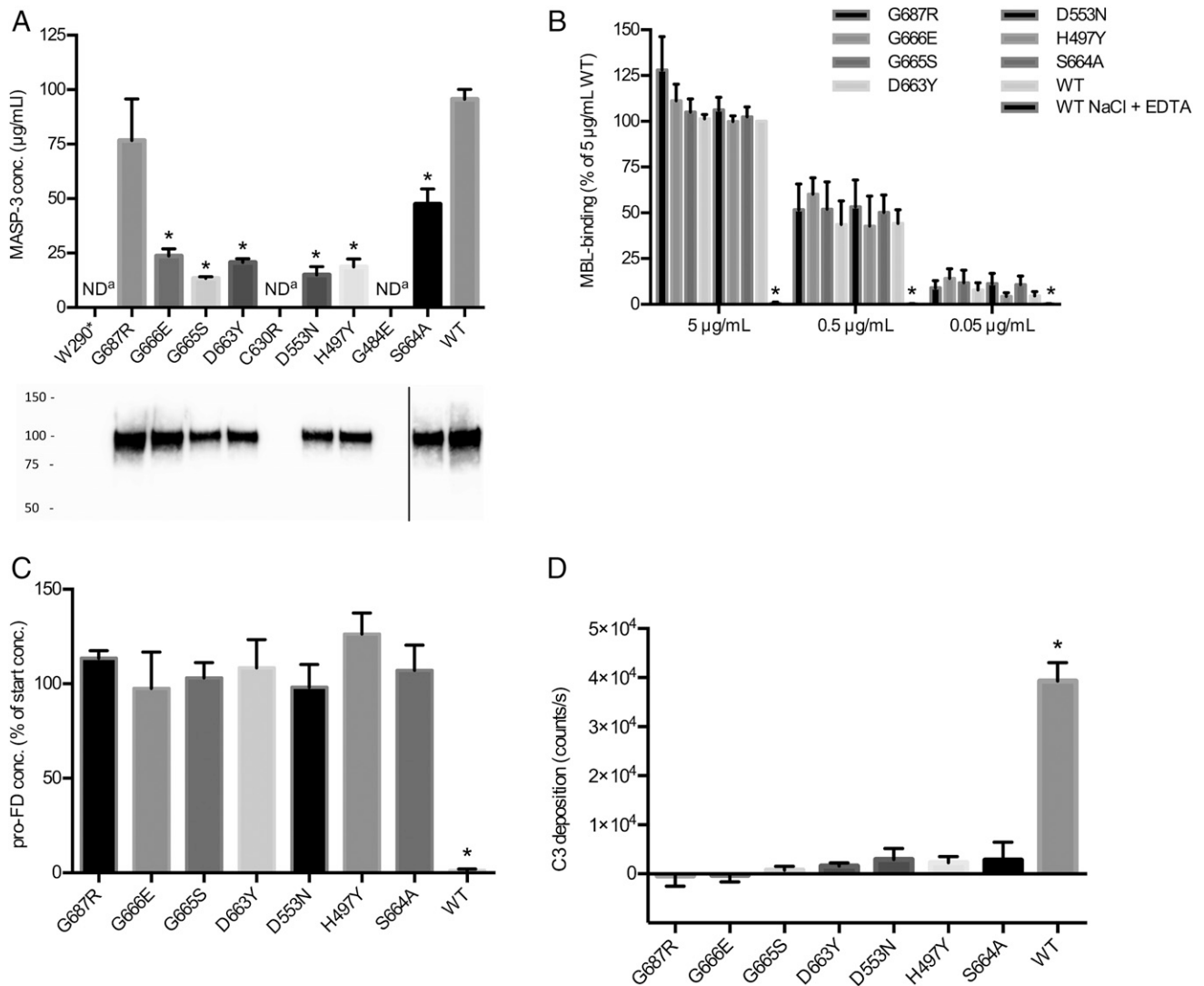
FIGURE 6. Characterization of 3MC MASP-3 mutants. (**A**) Expression levels of MASP-3 mutants in culture supernatants from transfected HEK293F cells. The immunoassay measurements were further supported by WB analysis of the supernatants using a polyclonal anti–MASP-3 Ab. The black line indicates where parts of the image were joined. The blot is representative of three repeated analyses. The concentrations were measured in the MASP-3 immunoassay, and the expression levels of the mutants were compared with that of MASP-3 WT by unpaired parametric t tests. *$p < 0.02$ ($n = 3$). (**B**) MBL-binding by MASP-3 mutants. Three different concentrations of the MASP-3 variants were incubated in wells containing immobilized MBL, and the amount of bound MASP-3 was detected using an Ab against MASP-3. As a negative control, MASP-3 WT was incubated in a buffer containing 1 M NaCl and 10 mM EDTA to prevent MBL–MASP-3 binding. The signal from 5 μg/ml MASP-3 WT was defined as 100% binding. The amount of bound MASP-3 mutant was compared with that of MASP-3 WT for each MASP-3 concentration using unpaired parametric t tests. *$p < 0.03$ ($n = 3$). (**C**) Pro-FD cleavage by MASP-3 mutants. Biotinylated pro-FD was incubated with the MASP-3 proteins at 37°C. The data are shown as the percent of remaining pro-FD after 24 h relative to the starting concentration. Statistically significant conversion was identified by comparing the pro-FD levels with that of MASP-3 S664A using unpaired parametric t tests. *$p < 0.0003$ ($n = 3$). (**D**) Rescue of the C3 deposition ability of ΔFD/ΔMASP-3 serum by addition of MASP-3 mutants and pro-FD. MASP-3 supernatants and pro-FD were added to the depleted sera and incubated for 1.5 h at 37°C before transferring the samples to zymosan-coated wells. The deposition levels were compared with that of MASP-3 S664A by unpaired parametric t tests. *$p < 0.0004$ ($n = 3$).

be of physiological relevance (Supplemental Fig. 2). Moreover, we note that there are no reports of 3MC patients who suffer from infections by Gram-negative bacteria (28, 29, 37, 50), whereas FD-deficient patients are known to be prone to recurrent Gram-negative bacterial infections (14, 51–53). This may suggest that the MASP-3–independent maturation of pro-FD provides sufficient AP activity to protect against these pathogens. However, it should be stressed that the very low number of 3MC patients who lack MASP-3 activity (20 individuals in total) precludes a statistical analysis of whether MASP-3–deficient patients are more likely to develop infections than healthy individuals.

To further investigate the role of MASP-3 as the main physiological converter of pro-FD into FD, we generated serum lacking all

FD variants and MASP-3. This serum was analyzed using two techniques developed in this study, that is, IEF blotting (Fig. 3) and the immunoassay that monitors and quantifies the conversion of biotinylated pro-FD (Fig. 5). The importance of MASP-3 for pro-FD maturation was thus examined by comparing the cleavage of pro-FD in ΔFD/ΔMASP-3 and ΔFD/Iso serum. We find that the maturation of pro-FD is largely dependent on MASP-3, because ΔFD/Iso serum readily converted pro-FD, whereas ΔFD/ΔMASP-3 serum generated only minute amounts of FD upon longer incubation times (Figs. 3A, 5C). This is in agreement with a previous study in which endogenous MASP-3 was inhibited (35). The residual pro-FD–cleaving activity observed in ΔFD/ΔMASP-3 serum is likely reflecting the aforementioned MASP-3–indepen-

dent backup mechanism. However, we cannot exclude the possibility that MASP-3 was not completely removed, because the MASP-3 immunoassay that is used to assess the depletion has a detection limit of 50 ng/ml. One limitation of our study is that MASP-1 and MAp44 were removed together with MASP-3 from ΔFD/ΔMASP-3 serum, which potentially complicates the interpretation of the MASP-3–mediated effect. Nevertheless, the fact that pro-FD conversion in ΔFD/ΔMASP-3 serum could be fully rescued by the addition of MASP-3 infers that the observed effects are indeed MASP-3 specific (Fig. 3). This is further supported by a study that showed that MASP-1 inhibition had no effect on pro-FD cleavage (34). Lastly, the key role of MASP-3 is highlighted by the fact that recombinant MASP-3 converted the endogenous pro-FD in 3MC serum into mature FD (Fig. 2C).

In addition, we find that the MASP-3–mediated generation of FD translates into AP activity. Both C3 deposition on the AP activator zymosan and lysis of rabbit erythrocytes were largely absent in ΔFD/ΔMASP-3 serum after addition of pro-FD. Again, a clear rescuing effect was observed when recombinant MASP-3 was added to the depleted serum (Fig. 3B, 3C). To further strengthen the biological relevance of these observations, we examined the effect of MASP-3 on the AP activity in $Masp1/3^{-/-}$ mice. Under the chosen experimental conditions, the AP activity in EDTA plasma from $Masp1/3^{-/-}$ mice was <10% of that of normal C57BL/6 mice. However, a fully functional AP was observed 4 and 24 h after i.v. injection of recombinant murine MASP-3 (Fig. 4). The AP activity returned to the baseline level after 1 wk when MASP-3 had been catabolized (data not shown). Thus, to our knowledge, we provide the first in vivo demonstration of the intimate link between MASP-3 activity and the AP.

It has been proposed that murine zymogenic MASP-3 possesses a pro-FD–cleaving activity that could be responsible for the continuous maturation of pro-FD in the circulation (33). In contrast, a study reported that a zymogenic fragment of human MASP-3 consisting of the CCP1-CCP2-SP domains did not cleave pro-FD (34). In this study, we used the zymogenic MASP-3 R449Q mutant in the assay for pro-FD cleavage and found that this variant of human full-length MASP-3 was not capable of cleaving pro-FD (Fig. 5B). It should be noted that we cannot exclude that the murine and human MASP-3 differ in respect to their zymogenicity. This indicates that the effects that are observed using recombinant MASP-3 in this study are caused by the low degree of activation that occurs during synthesis and purification of MASP-3 (Supplemental Fig. 1). Consequently, MASP-3 must be activated in vivo to generate mature FD, as inferred previously (34). Because the ratio between activated and zymogen MASP-3 in the circulation was unknown, we affinity-purified MASP-3 from EDTA plasma and used Western blotting to show that ~40% of circulating MASP-3 is found in the activated state (Supplemental Fig. 4). The original isolation of MASP-3 from plasma identified only the B chain, indicating that all MASP-3 was active (25). However, this was performed by isolating MBL–MASP complexes using mannan-Sepharose, thus leading to juxtaposition of MBL–MASP-3 complexes and MASP-1– and MASP-2–containing complexes. This may lead to activation, because MASP-1 and MASP-2 have been shown to be able to activate MASP-3 (33, 54). The activational state of MASP-3 contrasts those of MASP-1 and MASP-2, because they have both been purified as zymogens from serum (55). This explains why only MASP-3 is a physiological pro-FD maturase under resting condition, despite the fact that all MASPs are capable of cleaving pro-FD in vitro (34, 35).

The pro-FD conversion immunoassay was further used to follow pro-FD cleavage temporally, which enabled us to quantify the $conv_{1/2}$. Pro-FD was found to be converted with a $conv_{1/2}$ of 2.6 h in NHS (Fig. 5D), whereas the rate was found to be slightly lower in EDTA plasma ($conv_{1/2}$ = 3.3 h). These findings are remarkably consistent with the $conv_{1/2}$ values estimated by others using in-gel fluorescence to monitor the cleavage of Cy3-labeled pro-FD (2.2 h for serum and 3.8 h for EDTA plasma) (35).

Another key finding in our study is the presence of pro-FD in blood samples from healthy donors (Fig. 2A, Supplemental Fig. 3). This challenges the perception that FD exclusively circulates in its mature form (19, 20, 23) and instead supports the finding that there exists a FD precursor pool in serum (18). The nature of the pro-FD band in the IEF blots is verified by the following observations: 1) the position of the band matched that of recombinant pro-FD (Fig. 2B); 2) the band was recognized by a pro-FD-specific Ab (Fig. 2B); 3) the protein was identified as a 25-kDa protein by two-dimensional blotting (Fig. 1C); and 4) the position of the band in NHS matched that of the dominant FD species in 3MC sera, which is acknowledged as being pro-FD (Fig. 1B, 1C) (39). Furthermore, we note that the pro-FD/FD ratio varied significantly between individuals, with some donors containing comparable amounts of the isoforms, whereas others primarily have mature FD. Although pro-FD and FD were the major variants detected by IEF blotting, we recognize that unidentified FD species were also present (Figs. 1B, 2A). We do not regard this as an artifact, because these bands were absent in FD-depleted serum (Fig. 1B). This is further supported by reports of FD heterogeneity in the literature. A proteomic examination of uremic plasma from renal failure patients identified several FD species with differing pI values (56). Likewise, a variant of FD containing a short dipropeptide has been identified (20).

We suggest that the hitherto elusive nature of circulating pro-FD is primarily caused by two circumstances. First, purification of FD from human sources always includes at least one (and often several) ion exchange chromatography step (19, 20, 57–59). Due to the pI difference that we exploit in this study, it is likely that pro-FD is separated from mature FD during these procedures. Second, there has been a tradition for using activity assays to identify FD-containing fractions during purification, which biases the procedure toward FD (58, 59). In addition, we found that we were not able to convert the endogenous pro-FD into FD in our in vitro experiments (Fig. 2D). The underlying basis hereof is not yet known, but we note that a similar observation has been made in a murine system. In a study using cartilage microparticles as an activating surface, MASPs secreted from cultivated fibroblast-like synoviocytes were capable of cleaving pro-FD synthesized by cultured differentiated adipocytes, whereas the secreted MASPs did not convert the endogenous pro-FD in $Masp1/3^{-/-}$ serum into FD (60).

Lastly, we examined the molecular manifestations of the MASP-3 mutations that have been found in 3MC patients. Although these mutations have been predicted to have deleterious consequences for MASP-3 function by various software tools (27–29, 37, 50), few effects have been investigated experimentally. We showed that missense mutations C630R, D553N, and G484E block MASP-3 expression in HEK293 cells, which is most likely due to misfolding and intracellular degradation. All expressing mutants, except for G687R, were produced at a lower level than the WT protein (Fig. 6A). In the case of the novel G665S mutant, this is in agreement with the rather low level of circulating MASP-3 detected in the patient (3.7 μg/ml). Furthermore, we found that the expressing mutants display MBL-binding properties similar to the WT (Fig. 6B). The mutants G666E and G687R are the only variants that have previously been tested for enzymatic activity. This was performed using a synthetic tripeptide substrate, and the mutants were found to be inactive (27). The identification of pro-FD as a natural MASP-3 substrate permits the enzymatic properties of the 3MC variants to be investigated in a biologically

relevant context. We show that none of the MASP-3 mutants were capable of converting pro-FD or rescuing AP activity in ΔFD/ΔMASP-3 serum (Fig. 6C, 6D), in accordance with the in silico predictions. These results, and the finding that 3MC sera mainly contain pro-FD, underline the connection between MASP-3 and the AP.

In conclusion, IEF blotting proved to be a strong analytical tool for detecting the FD isoform distribution within complex samples. Using this approach, we show that MASP-3 is the principal maturase responsible for converting pro-FD into FD. However, minor levels of FD are still detected in 3MC patients. This highlights that small amounts of pro-FD are still cleaved through a MASP-3–independent mechanism, thereby resolving previous discrepancies in the literature. Furthermore, we find that pro-FD is also present in blood samples from healthy donors. Due to the increasing interest in FD as a drug target in autoimmune diseases, it is of central importance to understand the process of pro-FD maturation, because it could suggest novel strategies for therapeutic intervention (61, 62).

References

1. Merle, N. S., R. Noe, L. Halbwachs-Mecarelli, V. Fremeaux-Bacchi, and L. T. Roumenina. 2015. Complement system part II: role in immunity. *Front. Immunol.* 6: 257.
2. Holers, V. M. 2008. The spectrum of complement alternative pathway-mediated diseases. *Immunol. Rev.* 223: 300–316.
3. Degn, S. E., J. C. Jensenius, and M. Bjerre. 2011. The lectin pathway and its implications in coagulation, infections and auto-immunity. *Curr. Opin. Organ Transplant.* 16: 21–27.
4. Ricklin, D., E. S. Reis, and J. D. Lambris. 2016. Complement in disease: a defence system turning offensive. *Nat. Rev. Nephrol.* 12: 383–401.
5. Morgan, B. P., and C. L. Harris. 2015. Complement, a target for therapy in inflammatory and degenerative diseases. *Nat. Rev. Drug Discov.* 14: 857–877.
6. Degn, S. E., T. R. Kjaer, R. T. Kidmose, L. Jensen, A. G. Hansen, M. Tekin, J. C. Jensenius, G. R. Andersen, and S. Thiel. 2014. Complement activation by ligand-driven juxtaposition of discrete pattern recognition complexes. *Proc. Natl. Acad. Sci. USA* 111: 13445–13450.
7. Kjaer, T. R., T. M. Le, J. S. Pedersen, B. Sander, M. M. Golas, J. C. Jensenius, G. R. Andersen, and S. Thiel. 2015. Structural insights into the initiating complex of the lectin pathway of complement activation. *Structure* 23: 342–351.
8. Héja, D., A. Kocsis, J. Dobó, K. Szilágyi, R. Szász, P. Závodszky, G. Pál, and P. Gál. 2012. Revised mechanism of complement lectin-pathway activation revealing the role of serine protease MASP-1 as the exclusive activator of MASP-2. *Proc. Natl. Acad. Sci. USA* 109: 10498–10503.
9. Pangburn, M. K., R. D. Schreiber, and H. J. Müller-Eberhard. 1981. Formation of the initial C3 convertase of the alternative complement pathway. Acquisition of C3b-like activities by spontaneous hydrolysis of the putative thioester in native C3. *J. Exp. Med.* 154: 856–867.
10. Harboe, M., G. Ulvund, L. Vien, M. Fung, and T. E. Mollnes. 2004. The quantitative role of alternative pathway amplification in classical pathway induced terminal complement activation. *Clin. Exp. Immunol.* 138: 439–446.
11. White, R. T., D. Damm, N. Hancock, B. S. Rosen, B. B. Lowell, P. Usher, J. S. Flier, and B. M. Spiegelman. 1992. Human adipsin is identical to complement factor D and is expressed at high levels in adipose tissue. *J. Biol. Chem.* 267: 9210–9213.
12. Cook, K. S., D. L. Groves, H. Y. Min, and B. M. Spiegelman. 1985. A developmentally regulated mRNA from 3T3 adipocytes encodes a novel serine protease homologue. *Proc. Natl. Acad. Sci. USA* 82: 6480–6484.
13. Rosen, B. S., K. S. Cook, J. Yaglom, D. L. Groves, J. E. Volanakis, D. Damm, T. White, and B. M. Spiegelman. 1989. Adipsin and complement factor D activity: an immune-related defect in obesity. *Science* 244: 1483–1487.
14. Sprong, T., D. Roos, C. Weemaes, C. Neeleman, C. L. Geesing, T. E. Mollnes, and M. van Deuren. 2006. Deficient alternative complement pathway activation due to factor D deficiency by 2 novel mutations in the complement factor D gene in a family with meningococcal infections. *Blood* 107: 4865–4870.
15. Xu, Y., M. Ma, G. C. Ippolito, H. W. Schroeder, Jr., M. C. Carroll, and J. E. Volanakis. 2001. Complement activation in factor D-deficient mice. *Proc. Natl. Acad. Sci. USA* 98: 14577–14582.
16. Song, N. J., S. Kim, B. H. Jang, S. H. Chang, U. J. Yun, K. M. Park, H. Waki, D. Y. Li, P. Tontonoz, and K. W. Park. 2016. Small molecule-induced comple-

17. ment factor D (Adipsin) promotes lipid accumulation and adipocyte differentiation. *PLoS One* 11: e0162228.
17. Lo, J. C., S. Ljubicic, B. Leibiger, M. Kern, I. B. Leibiger, T. Moede, M. E. Kelly, D. Chatterjee Bhowmick, I. Murano, P. Cohen, et al. 2014. Adipsin is an adipokine that improves β cell function in diabetes. *Cell* 158: 41–53.
18. Fearon, D. T., K. F. Austen, and S. Ruddy. 1974. Properdin factor D: characterization of its active site and isolation of the precursor form. *J. Exp. Med.* 139: 355–366.
19. Lesavre, P. H., and H. J. Müller-Eberhard. 1978. Mechanism of action of factor D of the alternative complement pathway. *J. Exp. Med.* 148: 1498–1509.
20. Yamauchi, Y., J. W. Stevens, K. J. Macon, and J. E. Volanakis. 1994. Recombinant and native zymogen forms of human complement factor D. *J. Immunol.* 152: 3645–3653.
21. Kim, S., S. V. Narayana, and J. E. Volanakis. 1994. Mutational analysis of the substrate binding site of human complement factor D. *Biochemistry* 33: 14393–14399.
22. Jing, H., K. J. Macon, D. Moore, L. J. DeLucas, J. E. Volanakis, and S. V. Narayana. 1999. Structural basis of profactor D activation: from a highly flexible zymogen to a novel self-inhibited serine protease, complement factor D. *EMBO J.* 18: 804–814.
23. Volanakis, J. E., and S. V. Narayana. 1996. Complement factor D, a novel serine protease. *Protein Sci.* 5: 553–564.
24. Forneris, F., D. Ricklin, J. Wu, A. Tzekou, R. S. Wallace, J. D. Lambris, and P. Gros. 2010. Structures of C3b in complex with factors B and D give insight into complement convertase formation. *Science* 330: 1816–1820.
25. Dahl, M. R., S. Thiel, M. Matsushita, T. Fujita, A. C. Willis, T. Christensen, T. Vorup-Jensen, and J. C. Jensenius. 2001. MASP-3 and its association with distinct complexes of the mannan-binding lectin complement activation pathway. *Immunity* 15: 127–135.
26. Cortesio, C. L., and W. Jiang. 2006. Mannan-binding lectin-associated serine protease 3 cleaves synthetic peptides and insulin-like growth factor-binding protein 5. *Arch. Biochem. Biophys.* 449: 164–170.
27. Yongqing, T., P. G. Wilmann, S. B. Reeve, T. H. Coetzer, A. I. Smith, J. C. Whisstock, R. N. Pike, and L. C. Wijeyewickrema. 2013. The x-ray crystal structure of mannose-binding lectin-associated serine proteinase-3 reveals the structural basis for enzyme inactivity associated with the Carnevale, Mingarelli, Malpuech, and Michels (3MC) syndrome. *J. Biol. Chem.* 288: 22399–22407.
28. Sirmaci, A., T. Walsh, H. Akay, M. Spiliopoulos, Y. B. Şakalar, A. Hasanefendioğlu-Bayrak, D. Duman, A. Farooq, M. C. King, and M. Tekin. 2010. MASP1 mutations in patients with facial, umbilical, coccygeal, and auditory findings of Carnevale, Malpuech, OSA, and Michels syndromes. *Am. J. Hum. Genet.* 87: 679–686.
29. Rooryck, C., A. Diaz-Font, D. P. Osborn, E. Chabchoub, V. Hernandez-Hernandez, H. Shamseldin, J. Kenny, A. Waters, D. Jenkins, A. A. Kaissi, et al. 2011. Mutations in lectin complement pathway genes COLEC11 and MASP1 cause 3MC syndrome. *Nat. Genet.* 43: 197–203.
30. Titomanlio, L., S. Bennaceur, D. Bremond-Gignac, C. Baumann, O. Dupuy, and A. Verloes. 2005. Michels syndrome, Carnevale syndrome, OSA syndrome, and Malpuech syndrome: variable expression of a single disorder (3MC syndrome)? *Am. J. Med. Genet.* 137A: 332–335.
31. Munye, M. M., A. Diaz-Font, L. Ocaka, M. L. Henriksen, M. Lees, A. Brady, D. Jenkins, J. Morton, S. W. Hansen, C. Bacchelli, et al. 2017. COLEC10 is mutated in 3MC patients and regulates early craniofacial development. *PLoS Genet.* 13: e1006679.
32. Takahashi, M., Y. Ishida, D. Iwaki, K. Kanno, T. Suzuki, Y. Endo, Y. Homma, and T. Fujita. 2010. Essential role of mannose-binding lectin-associated serine protease-1 in activation of the complement factor D. *J. Exp. Med.* 207: 29–37.
33. Iwaki, D., K. Kanno, M. Takahashi, Y. Endo, M. Matsushita, and T. Fujita. 2011. The role of mannose-binding lectin-associated serine protease-3 in activation of the alternative complement pathway. *J. Immunol.* 187: 3751–3758.
34. Oroszlán, G., E. Kortvely, D. Szakács, A. Kocsis, S. Dammeier, A. Zeck, M. Ueffing, P. Závodszky, G. Pál, P. Gál, and J. Dobó. 2016. MASP-1 and MASP-2 do not activate pro-factor D in resting human blood, whereas MASP-3 is a potential activator: kinetic analysis involving specific MASP-1 and MASP-2 inhibitors. *J. Immunol.* 196: 857–865.
35. Dobó, J., D. Szakács, G. Oroszlán, E. Kortvely, B. Kiss, E. Boros, R. Szász, P. Závodszky, P. Gál, and G. Pál. 2016. MASP-3 is the exclusive pro-factor D activator in resting blood: the lectin and the alternative complement pathways are fundamentally linked. *Sci. Rep.* 6: 31877.
36. Degn, S. E., L. Jensen, A. G. Hansen, D. Duman, M. Tekin, J. C. Jensenius, and S. Thiel. 2012. Mannan-binding lectin-associated serine protease (MASP)-1 is crucial for lectin pathway activation in human serum, whereas neither MASP-1 nor MASP-3 is required for alternative pathway function. *J. Immunol.* 189: 3957–3969.
37. Atik, T., A. Koparir, G. Bademci, J. Foster, II, U. Altunoglu, G. Y. Mutlu, S. Bowdin, N. Elcioglu, G. A. Tayfun, S. S. Atik, et al. 2015. Novel MASP1 mutations are associated with an expanded phenotype in 3MC1 syndrome. *Orphanet J. Rare Dis.* 10: 128.
38. Ruseva, M. M., M. Takahashi, T. Fujita, and M. C. Pickering. 2014. C3 dysregulation due to factor H deficiency is mannan-binding lectin-associated serine proteases (MASP)-1 and MASP-3 independent in vivo. *Clin. Exp. Immunol.* 176: 84–92.
39. Takahashi, M., H. Sekine, and T. Fujita. 2014. Comment on "the pro-factor D cleaving activity of MASP-1/-3 is not required for alternative pathway function". *J. Immunol.* 192: 5448–5449.
40. Fenton, T. R., and J. H. Kim. 2013. A systematic review and meta-analysis to revise the Fenton growth chart for preterm infants. *BMC Pediatr.* 13: 59.

41. Mortensen, S. A., B. Sander, R. K. Jensen, J. S. Pedersen, M. M. Golas, J. C. Jensenius, A. G. Hansen, S. Thiel, and G. R. Andersen. 2017. Structure and activation of C1, the complex initiating the classical pathway of the complement cascade. *Proc. Natl. Acad. Sci. USA* 114: 986–991.

42. Jensenius, J. C., P. H. Jensen, K. McGuire, J. L. Larsen, and S. Thiel. 2003. Recombinant mannan-binding lectin (MBL) for therapy. *Biochem. Soc. Trans.* 31: 763–767.

43. Degn, S. E., L. Jensen, P. Gál, J. Dobó, S. H. Holmvad, J. C. Jensenius, and S. Thiel. 2010. Biological variations of MASP-3 and MAp44, two splice products of the MASP1 gene involved in regulation of the complement system. *J. Immunol. Methods* 361: 37–50.

44. Troldborg, A., A. Hansen, S. W. K. Hansen, J. C. Jensenius, K. Stengaard-Pedersen, and S. Thiel. 2017. Lectin complement pathway proteins in healthy individuals. *Clin. Exp. Immunol.* 188: 138–147.

45. Schindelin, J., I. Arganda-Carreras, E. Frise, V. Kaynig, M. Longair, T. Pietzsch, S. Preibisch, C. Rueden, S. Saalfeld, B. Schmid, et al. 2012. Fiji: an open-source platform for biological-image analysis. *Nat. Methods* 9: 676–682.

46. Tenner, A. J., P. H. Lesavre, and N. R. Cooper. 1981. Purification and radio-labeling of human C1q. *J. Immunol.* 127: 648–653.

47. Pedersen, D. V., L. Roumenina, R. K. Jensen, T. A. Gadeberg, C. Marinozzi, C. Picard, T. Rybkine, S. Thiel, U. B. Sørensen, C. Stover, et al. 2017. Functional and structural insight into properdin control of complement alternative pathway amplification. *EMBO J.* 36: 1084–1099.

48. Banda, N. K., S. Acharya, R. I. Scheinman, G. Mehta, M. Coulombe, M. Takahashi, H. Sekine, S. Thiel, T. Fujita, and V. M. Holers. 2016. Mannan-binding lectin-associated serine protease 1/3 cleavage of pro-factor D into factor D in vivo and attenuation of collagen antibody-induced arthritis through their targeted inhibition by RNA interference-mediated gene silencing. *J. Immunol.* 197: 3680–3694.

49. Degn, S. E., J. C. Jensenius, and S. Thiel. 2014. The pro-factor D cleaving activity of MASP-1/-3 is not required for alternative pathway function. *J. Immunol.* 192: 5447–5448.

50. Urquhart, J., R. Roberts, D. de Silva, S. Shalev, E. Chervinsky, S. Nampoothiri, Y. Sznajer, N. Revencu, R. Gunasekera, M. Suri, et al. 2016. Exploring the genetic basis of 3MC syndrome: findings in 12 further families. *Am. J. Med. Genet. A.* 170A: 1216–1224.

51. Kluin-Nelemans, H. C., H. van Velzen-Blad, H. P. van Helden, and M. R. Daha. 1984. Functional deficiency of complement factor D in a monozygous twin. *Clin. Exp. Immunol.* 58: 724–730.

52. Hiemstra, P. S., E. Langeler, B. Compier, Y. Keepers, P. C. Leijh, M. T. van den Barselaar, D. Overbosch, and M. R. Daha. 1989. Complete and partial deficiencies of complement factor D in a Dutch family. *J. Clin. Invest.* 84: 1957–1961.

53. Biesma, D. H., A. J. Hannema, H. van Velzen-Blad, L. Mulder, R. van Zwieten, I. Kluijt, and D. Roos. 2001. A family with complement factor D deficiency. *J. Clin. Invest.* 108: 233–240.

54. Megyeri, M., V. Harmat, B. Major, Á. Végh, J. Balczer, D. Héja, K. Szilágyi, D. Datz, G. Pál, P. Závodszky, et al. 2013. Quantitative characterization of the activation steps of mannan-binding lectin (MBL)-associated serine proteases (MASPs) points to the central role of MASP-1 in the initiation of the complement lectin pathway. *J. Biol. Chem.* 288: 8922–8934.

55. Matsushita, M., S. Thiel, J. C. Jensenius, I. Terai, and T. Fujita. 2000. Proteolytic activities of two types of mannose-binding lectin-associated serine protease. *J. Immunol.* 165: 2637–2642.

56. Ward, R. A., and K. A. Brinkley. 2004. A proteomic analysis of proteins removed by ultrafiltration during extracorporeal renal replacement therapy. *Contrib. Nephrol.* 141: 280–291.

57. Volanakis, J. E., and K. J. Macon. 1987. Isolation of complement protein D from urine of patients with Fanconi's syndrome. *Anal. Biochem.* 163: 242–246.

58. DiScipio, R. G. 1994. The fractionation of human plasma proteins. I. Affinity purification of human complement properdin. *Protein Expr. Purif.* 5: 164–169.

59. Johnson, D. M., J. Gagnon, and K. B. Reid. 1980. Factor D of the alternative pathway of human complement. Purification, alignment and N-terminal amino acid sequences of the major cyanogen bromide fragments, and localization of the serine residue at the active site. *Biochem. J.* 187: 863–874.

60. Arend, W. P., G. Mehta, A. H. Antonioli, M. Takahashi, K. Takahashi, G. L. Stahl, V. M. Holers, and N. K. Banda. 2013. Roles of adipocytes and fibroblasts in activation of the alternative pathway of complement in inflammatory arthritis in mice. *J. Immunol.* 190: 6423–6433.

61. Yang, C.Y., J. G. Phillips, J. A. Stuckey, L. Bai, H. Sun, J. Delproposto, W. C. Brown, and K. Chinnaswamy. 2016. Buried hydrogen bond interactions contribute to the high potency of complement factor D inhibitors. *ACS Med. Chem. Lett.* 7: 1092–1096.

62. Yuan, X., E. Gavriilaki, J. A. Thanassi, G. Yang, A. C. Baines, S. D. Podos, Y. Huang, M. Huang, and R. A. Brodsky. 2017. Small-molecule factor D inhibitors selectively block the alternative pathway of complement in paroxysmal nocturnal hemoglobinuria and atypical hemolytic uremic syndrome. *Haematologica* 102: 466–475.